View metadata, citation and similar papers at core.ac.uk

brought to you by CORE

provided by DigitalCommons@The Texas Medical Center

NIH Public Access
Author Manuscript
J Comp Neurol. Author manuscript; available in PMC 2010 June 28.

Published in final edited form as:
J Comp Neurol. 2008 October 10; 510(5): 550–559. doi:10.1002/cne.21806.

SYNTAXIN 3B IS A T-SNARE SPECIFIC FOR RIBBON SYNAPSES OF THE RETINA

LEIGH B. CURTIS[1], **BLAIR DONESKE**[2], **XIAOQIN LIU**[1], **CHRISTINA THALLER**[3], **JAMES A. MCNEW**[2], and **ROGER JANZ**[1]

Ian Meinertzhagen

[1]Department of Neurobiology and Anatomy, The University of Texas Medical School, Houston, Texas 77030

[2]Department of Biochemistry and Cell Biology, Rice University, Houston, TX, USA 77030

[3]Department of Biochemistry, Baylor College of Medicine, Houston, Texas, 77030

Abstract

Previous studies have demonstrated that ribbon synapses in the retina do not contain the t-SNARE (target-soluble *N*-ethylmaleimide-sensitive factor attachment protein receptor) syntaxin 1A that is found in conventional synapses of the nervous system. In contrast, ribbon synapses of the retina contain the related isoform syntaxin 3. In addition to its localization in ribbon synapses, syntaxin 3 is also found in non-neuronal cells, where it has been implicated in the trafficking of transport vesicles to the apical plasma membrane of polarized cells. The syntaxin 3 gene codes for four different splice forms, syntaxin 3A, 3B, 3C and 3D. We demonstrate here using analysis of EST databases, RT-PCR, *in situ* hybridization and Northern blot analysis that cells in the mouse retina only express syntaxin 3B. In contrast non-neuronal tissues, such as kidney express only syntaxin 3A. The two major syntaxin isoforms (3A and 3B) have an identical N-terminal domain but differ in the C-terminal half of the SNARE domain and the C-terminal transmembrane domain. These two domains are thought to be directly involved in synaptic vesicle fusion. The interaction of syntaxin 1A and syntaxin 3B with other synaptic proteins was examined. We found that both proteins bind Munc18/N-sec1 with similar affinity. In contrast, syntaxin 3B had a much lower binding affinity for the t-SNARE SNAP-25 compared to that of syntaxin1A. Using an *in vitro* fusion assay we could demonstrate that vesicles containing syntaxin 3B and SNAP-25 could fuse with vesicles containing synaptobrevin2/VAMP2, demonstrating that syntaxin 3B can function as a t-SNARE.

Keywords

vesicle fusion; SNAP-25; Synaptobrevin; VAMP; splicing; isoform

INTRODUCTION

Ribbon synapses are a specialized type of synapse found in photoreceptors and bipolar cells of the retina, hair cells of the inner ear, and pinealocytes of the pineal gland. In contrast to conventional synapses, which release neurotransmitter phasically, ribbon synapses tonically release large amounts of neurotransmitter (Sterling and Matthews, 2005; Heidelberger et al., 2005). Despite these differences in the physiology of neurotransmitter release,

Address correspondence to: Roger Janz, Department of Neurobiology and Anatomy, UT Houston Medical School, Houston, 6431 Fannin, Houston TX 77030, Tel.: 713-500-5634, FAX: 713-500-0621, Roger.Janz@uth.tmc.edu.

NIH-PA Author Manuscript

NIH-PA Author Manuscript

NIH-PA Author Manuscript

NIH-PA Author Manuscript

NIH-PA Author Manuscript

NIH-PA Author Manuscript

neurotransmitters are released by Ca2+ dependent exocytosis of synaptic vesicles in both types of synapses. Fusion of synaptic vesicles with the presynaptic plasma membrane in conventional synapses is dependent upon a set of SNARE (soluble N-ethylmaleimide-sensitive factor attachment protein receptor) proteins (Jahn and Scheller, 2006). SNAREs participate in membrane trafficking in eukaryotic cells. These proteins are localized within the cell to transport vesicle membranes, subcellular compartment membranes, and the cytoplasmic side of the plasma membrane. SNAREs are classified according to the membrane in which they primarily reside. Vesicle membrane SNAREs are referred to as v-SNAREs and target membrane SNAREs are referred to as t-SNAREs. In conventional synapses, synaptic vesicle fusion is dependent upon the synaptic vesicle associated v-SNARE protein synaptobrevin 2 (also called VAMP2) and the plasma membrane associated t-SNARE proteins syntaxin 1A and SNAP-25. These three proteins form a trimeric complex that is thought to be involved in the correct targeting of vesicles to the synaptic plasma membrane as well as play a role in the fusion reaction. The synaptic vesicle fusion reaction is thought to be regulated by interactions between the SNARE complex and synaptic proteins such as Munc18/N-sec1, synaptotagmin and the complexins.

In addition to a central role for syntaxin 1A in synaptic vesicles fusion, this protein has also been implicated in an interaction with voltage-gated calcium channels, suggesting a role for syntaxin 1A in regulation of the localization and activity of these ion channels (Sheng et al., 1994; Catterall, 1999; Arien et al., 2003). Recently, interactions between syntaxin 1A and other ion channels have also been described (Fili et al., 2001; Singer-Lahat et al., 2007).

Ribbon synapses in the retina contain SNAP-25 and synaptobrevin2/VAMP2 but they do not contain syntaxin 1A (Brandstätter et al., 1996). Instead, they contain the related isoform syntaxin 3 (Morgans et al., 1996; Sherry et al., 2006). Besides its presumed role in synaptic vesicle fusion in ribbon synapses in the retina, syntaxin 3 has also recently been implicated in the trafficking of rhodopsin in rod photoreceptors (Chuang et al., 2007). In contrast to its expression in photoreceptors and bipolar cells, syntaxin 3 is not found in conventional synapses in the retina and is also not detectable in the brain using Northern or Western blot analysis (Bennett et al., 1993; Morgans et al., 1996; Sherry et al., 2006). However, syntaxin 3 is expressed at high levels in non-neuronal tissues like spleen, lung and kidney (Bennett et al., 1993). In polarized epithelial cells syntaxin 3 has been shown to be involved in the trafficking of vesicles from the trans-Golgi to the apical plasma membrane (Low et al., 1998).

Originally, only one form of syntaxin 3 was isolated (Bennett et al., 1993), but further screening of brain cDNA libraries from mouse brain lead to the isolation of cDNA clones coding for three other syntaxin isoforms called syntaxin 3B, 3C and 3D (Ibaraki et al., 1995). The isoform that was first isolated is consequently referred to as syntaxin 3A. The four syntaxin 3 isoforms differ in their domain structure and biochemical properties (Ibaraki et al., 1995). The distribution of these isoforms in different cell types has not been investigated. Specifically, the syntaxin 3 isoform found in ribbon synapses of the retina has not been previously characterized.

MATERIALS AND METHODS

Animals

Adult C57BL6 mice were euthanized using CO_2 using a protocol approved by the animal welfare committee of the UT Houston Medical School. Tissues were then dissected out and processed for the different procedures.

NIH-PA Author Manuscript

NIH-PA Author Manuscript

NIH-PA Author Manuscript

Bioinformatics

EST database searches were performed using the BLAST program suite at the NCBI website. The protein sequences were aligned using the ClustalW and Boxshade programs using default settings at the Biology Workbench (http://workbench.sdsc.edu/).

GST (Glutathione S-transferase) pulldown

GST fusion proteins were expressed in Escherichia coli BL21 cells and purified using gluthathione-sepharose beads. Mouse retinas were homogenized in buffer A consisting of 20 mM Hepes-NaOH pH 7.4, 0.2 mM PMSF, 2μg/ml aprotinin, 2μg/ml pepstatin, and 2μg/ml leupeptin. After homogenization, an equal amount of buffer B (20 mM Hepes-NaOH pH 7.4, 0.2 M NaCl, 2% Triton X-100) was added and the homogenate was incubated at 4°C with rotation for 30 min. The homogenate was then centrifuged for 1 hr at 20000 rpm at 4° C in a JA-20 rotor and the supernatant used for binding experiments. The protein concentration in the supernatant was adjusted by dilution to 0.1 mg/ml. Binding reactions were performed with 150 μM CaCl or 2 mM EGTA. One ml of the extract was mixed with the glutathione-sepharose beads for each binding reaction. The samples were then incubated overnight at 4°C with rotation. After overnight incubation, the samples were centrifuged at 3000 rpm for 30 seconds. The supernatant was removed and the beads were washed 6 times with cold wash buffer (20 mM Hepes-NaOH pH 7.4, 0.1 M NaCl, 1% Triton X-100) with either 150 μM CaCl2 or 2 mM EGTA. After the washes, SDS reducing sample buffer was added and the samples were analyzed by SDS-PAGE and western blotting.

In situ hybridization

Mouse cDNA clones coding for syntaxin 3A (image clone number: 3465516) and syntaxin 3B (accession number: BC024844, IMAGE clone number: 5357204) were used to generate digoxigenin-labeled sense and antisense RNA probes using the kits from Roche. Antisense probes containing the divergent C-terminal coding region and the 3' untranslated region were generated from SacI cut plasmids and *in vitro* translation using T7 RNA polymerase. Full-length sense control probes were generated in a similar way using EcoR1 (syntaxin 3A) and Not I (syntaxin 3B) cut plasmids and T3 (Syntaxin 3A) and SP6 (Syntaxin 3B) RNA polymerase. The probes were then used for *in situ* hybridization of 16 μm cryosections from paraformaladehyde fixed mouse retina as previously described (Belizaire et al., 2004; Yaylaoglu et al., 2005). Digital bright field images were captured from an Olympus BX51 upright microscope using an Olympus DP70 CCD camera with Olympus DPC controller software. The figure was generated using Adobe Photoshop CS3 10.0 and Adobe Illustrator CS3 13.0 (San Jose, CA) without changing the contrast or the intensity of the original images.

In vitro fusion assay

Full-length syntaxin1A (rat) and His_6SNAP25b (mouse) from plasmid pTW38 and VAMP2-His6 (mouse) from pTW38 were expressed and purified as previously described (Parlati et al., 1999). Full length syntaxin3b (mouse) from plasmid pJM485 and His_6SNAP25b (mouse) from plasmid pFP247 were co-expressed in BL21 (DE3) and purified by metal chelate chromatography on an ÄKTAprime liquid chromatography system (Amersham). The purified syntaxin1A/SNAP25 (syn1a/SN25) and the syntaxin3B/SNAP25 (syn3b/SN25) complexes were then each mixed, (250μl (~1,400 μg) and 125μl (~638 μg) of protein respectively) with A100 buffer (25mM HEPES-KOH, pH 7.4, 100mM KCl, 10% (w/v) glycerol), 1% OG) to a final volume of 1ml and used to resuspend a lipid film of 1.5 μmole 1-palmitoyl-2-dioleoyl-sn-glycero-3-phosphatidylcholine: 1,2-dioleoyl-sn-glycero-3-phosphatidylserine (POPC:DOPS) in an 85:15 mole ratio. The neuronal v-SNARE VAMP2 (50μl, ~275 μg protein) was mixed with 50μl A100 buffer, 1% OG and used to resuspend a

NIH-PA Author Manuscript

NIH-PA Author Manuscript

NIH-PA Author Manuscript

lipid film of 300 nmole POPC:DOPS:Rh-DPPE (1,2-dioleoyl-sn-glycero-3-phosphoethanolamine-N-(lissamine rhodamine B sulfonyl):NBD-DPPE (1,2-Dioleoyl-sn-Glycero-3-phosphoethanol-amine-N-(7-nitro-2-1,3-benzoxadiazol-4-yl)) in a 82:15:1.5:1.5 mole ratio. Liposomes were formed by detergent dilution and dialysis and isolated by flotation in a discontinuous Accudenz step gradient (Accurate Chemicals) in A100 buffer with 1 mM DTT as previously described (Weber et al., 1998; Scott et al., 2003). Proteoliposomes were harvested from the 30-0% interface (400μl for t-SNARE liposomes and 150μl for v-SNARE liposomes). Protein concentration in liposomes was determined by an amido black protein assay and ranged from 0.34 to 0.51 mg/ml for syntaxin1a/SNAP25 liposomes, 0.50-0.71 mg/ml for syntaxin3b/SNAP25 liposomes, and 0.64 mg/ml for VAMP2 liposomes. Lipid recovery was determined by tracer 3H-DPPC following flotation and was ~78-82% for syntaxin1a/SNAP25 liposomes, ~81-88% for syntaxin 3B/SNAP25 liposomes and ~72-85% for synaptobrevin 2 liposomes. Fusion assays were performed as previously described (Weber et al., 1998; Scott et al., 2003) with the following modifications. All assays included 45 μl t-SNARE liposomes and 5 μl v-SNARE. All components were mixed in a 96-well Fluoronunc polysorp plate (Nunc) on ice and incubated overnight at 4°C. The plate was then removed from 4°C and immediately placed in a 37°C fluorescent plate reader (Floroskan II, Labsystems). NBD fluorescence was measured (excitation 460 nm, emission 538 nm) at 2 min intervals for 120 min at which time 10 μl of 2.5% (w/v) n-dodecylmaltoside (Roche) was added to determine absolute NBD fluorescence. The kinetic data was normalized as a percent of total fluorescence as previously described (Parlati et al., 1999; Scott et al., 2003).

Northern Blot

Total RNA from mouse retina, brain, liver, and kidney was isolated using standard procedures as described for RT-PCR. The Northern blot and hybridization was performed using the NorthernMax Kit (Ambion) according to the manufacturer's protocol. A Sac I/NotI fragment from the mouse syntaxin 3B EST clone corresponding to the 3’ untranslated region of the syntaxin 3B mRNA was used for the hybridization. The probe was radioactively labeled using the Random Prime Labeling kit from Roche.

Plasmid Construction

A Mouse EST clone (accession number: BC024844, IMAGE clone number: 5357204) coding for full length syntaxin3B was used as a template to generate syntaxin 3B expression constructs by PCR. The syntaxin3B GST fusion construct (pGST-sytx3B) was generated by cloning the region coding for the cytoplasmic domain without the transmembrane domain (residues 2-264) into the pGEX-KG expression vector using BamHI and EcoRI. For the full length expression construct (pJM485) the coding region of syntaxin 3B was cloned using Nco I and BamH I into pET28a (Novagen). All constructs were verified by direct sequencing of the generated plasmids. The syntaxin 1 GST fusion construct containing the cytoplasmic domain without the transmembrane domain (residues 4-267) have been described before by Pevsner et al. (Pevsner et al., 1994a). The clones pTW34, pTW38 and pFP247 were previously described by Parlati et al. (Parlati et al., 1999).

Reverse Transcription Polymerase Chain Reaction (RT-PCR)

Total RNA was isolated from tissue of C57BL6 mice with Trizol reagent (Invitrogen) using the manufacturer's protocol. cDNA was generated using the Transcriptor First strand cDNA Synthesis kit (Roche). Two micrograms of total RNA from each tissue was used in this reaction. The synthesized cDNA was then used for PCR. PCR products were separated on a 3.0% agarose gel. After visualization, the products were isolated from the gel, purified and sequenced by Seqwright (Houston, TX).

NIH-PA Author Manuscript

NIH-PA Author Manuscript

NIH-PA Author Manuscript

Primer sequences:

Syntaxin 3A

Exon 8 sense: GTTTATGGACATCGCCATGCTGGTGGAA.

Exon 10A antisense: CCCAGCAACACAACTACTACCACAATGA.

Syntaxin 3B

Exon 8 sense: GTTTATGGACATCGCCATGCTGGTGGAA.

Exon 11B antisense: AACAGTTGATTGGTGCCCTGTGTTGTGA.

Syntaxin 3C/D

Exon 2 sense: CCTTCATGGACGAGTTCTTCTCT

Exon 4 antisense TCTTGATCTCAGTTGTGAGCTGTT.

GAPDH: ATGACATCAAGAAGGTGGTG and CATACCAGGAAATGAGCTTG.

Western Blotting

Primary antibodies used were SNAP-25 (Cl 71.1) 1:10,000 from Synaptic Systems (Göttingen, Germany) and Munc-18 (clone 31) 1:5000 from BD Transduction Labs. The SNAP-25 antibody has been raised against full length recombinant rat SNAP-25B His6 fusion protein (Bruns et al., 1998). It recognizes an epitope between position amino acid 20 to 40 that is conserved between the splice forms SNAP-25 A and B from rat and mouse (information from manufacturer). A specific band of approximately 25 kD was detected using western blot analysis of mouse brain or retina extract in our lab. The Munc-18 monoclonal antibody was raised against a recombinant protein containing amino acids 381 -567 of the rat munc-18 (information from manufacturer). The specificity of the Munc-18 antibody for mouse tissue has been previously demonstrated (Verhage et al., 2000) using western blot analysis of brain extracts from munc-18 knockout mice. A specific band of approximately 68 kD was detected using western blot analysis of mouse brain or retina extract in our lab. The secondary antibody used was HRP goat anti-mouse from Zymed. Blots were developed using ECL plus kit from Amersham.

RESULTS

Syntaxin 3 isoforms are generated by differential splicing of the syntaxin 3 gene

Full length cDNA clones coding for syntaxin 3A, 3BC and 3C as well as a partial clone coding for syntaxin 3B have been previously isolated from mouse brain (Ibaraki et al., 1995). We screened the mouse EST database and identified a cDNA clone that contained an open reading frame coding for a full-length syntaxin 3B (IMAGE clone number: 5357204). When the cDNA sequences coding for the four different syntaxin 3 isoforms were compared with that of the mouse genome sequence a single copy gene that codes for all four different syntaxin 3 isoforms was identified.

The four different isoforms of syntaxin 3 are generated by differential splicing. The exonintron structure of the gene and the corresponding splice forms are depicted in figure 1. The N-termini of syntaxin 3A and 3B are identical generated by the splicing of exons 1 to 8. In contrast, the C-termini of syntaxin 3A and 3B differ and are generated by the splicing of three different exons, 9A/B, 10A/B and 11A/B. As a consequence of this differential

NIH-PA Author Manuscript

NIH-PA Author Manuscript

NIH-PA Author Manuscript

splicing the second half of the SNARE domains as well as the C-terminal trans-membrane domains are different between syntaxin 3A and 3B. The syntaxin 3C isoform is almost identical to syntaxin 3B, except its transcript contains the exon 3C instead of the exon 3AB. In contrast, syntaxin 3D is generated by splicing together exons 3AB and 3C. This splicing leads to a frame shift of the coding region, resulting in a stop codon at the beginning of exon 3C and subsequently, a truncated protein.

Tissue-distribution of the different syntaxin 3 isoforms

In order to analyze the tissue distribution of the four different syntaxin 3 isoforms, mouse EST libraries were searched for the presence of the different syntaxin 3 isoforms. We used BLAST to search the existing mouse EST databases for sequences corresponding to the different syntaxin 3 isoforms. We identified 11 EST sequences containing the specific coding region for syntaxin 3A. The majority of the syntaxin 3A ESTs were derived from cDNA libraries generated from mammary gland/mammary gland tumors (5 clones) and thymus (3). No syntaxin 3A ESTs from cDNA libraries of neuronal tissues, retina or eyes were found. In contrast, 11 syntaxin 3B ESTs were identified that were all derived from cDNA libraries from retina or whole eye. One syntaxin 3B EST was identified that derived from a mammalian tumor library, but that clone seemed to be fused. Searches for syntaxin 3C did not identify any ESTs. Three ESTs from a brain cDNA library were identified using a syntaxin 3D probe. These findings suggesr that syntaxin 3B is the isoform that is most likely to be expressed in the retina. In order to confirm the hypothesis that syntaxin 3B is the isoform expressed in the retina, RNA was isolated from mouse retina, brain and kidney, and RT-PCR analysis was performed.

Specific primers were designed to amplify the different syntaxin 3 isoforms. The sequences of all generated PCR products were confirmed by direct sequencing. The results of the experiments are depicted in figure 2. Primers derived from exon 8 and exon 10A were used to identify the presence of syntaxin 3A mRNA. Syntaxin 3A was not detectable in the retina, weakly expressed in the brain and strongly expressed in the kidney. Primers derived from exons 8 and exon 11B were used to detect both syntaxin 3B and 3C, since the C-termini of syntaxin 3B and syntaxin 3C are identical. The analysis revealed a high level of expression of syntaxin 3B/C in the retina, a low level of expression in the brain, and no detectable expression in the kidney. In order to distinguish between the expression of syntaxin 3B and syntaxin 3C, primers located in exon 2 and 4 were used. This PCR reaction generated three different-sized products specific for syntaxin 3A/B, syntaxin 3C and syntaxin 3D. A PCR product specific for syntaxin 3A/B was detected in the retina. No signal was detected for syntaxin 3C or syntaxin 3D in the retina. In the brain, PCR products were produced for syntaxin 3A/B, 3C and 3D at approximately equivalent low levels. In the kidney, only a PCR product specific for syntaxin A/B was detectable.

Results of the EST database searches, combined with the RT-PCR data, resulted in distinct expression patterns for the four syntaxin isoforms. These data indicate that syntaxin 3B is the only isoform expressed in the retina. All four syntaxin isoforms were detectable in the brain but probably expressed at low levels. This conclusion is consistent with the isolation of cDNA clones coding for the four isoforms from libraries derived from mouse brain (Ibaraki et al., 1995). Syntaxin 3A is the only isoform that is detectable in the kidney. This isoform is expressed at high levels. This result indicates that syntaxin 3A is the major isoform expressed in non-neuronal tissues consistent with the tissue origin of the syntaxin 3A EST clones.

In order to compare the levels of syntaxin 3B mRNA expression in the retina with other tissues, we performed Northern blot analysis using a probe from the 3' untranslated region of the syntaxin 3B cDNA (Fig. 3). A signal corresponding to a message of approximately 3kB

NIH-PA Author Manuscript

NIH-PA Author Manuscript

NIH-PA Author Manuscript

was seen in the retina (lane 1). No specific signal was detected in the brain, liver or kidney (lanes 2 to 4). These data indicate that, in contrast to the retina, syntaxin 3B is expressed only at very low levels in the brain, since it can only be detected with RT-PCR. This experiment also confirms that the syntaxin 3B isoform is not expressed in non-neuronal tissue.

Syntaxin 3 protein is found in all ribbon synapses of the retina. This type of synapse in the retina is formed by rod and cone photoreceptors, as well as by bipolar neurons. Since syntaxin 3B is the major isoform expressed in the retina, the mRNA should therefore be expressed by photoreceptors and bipolar neurons. Expression of syntaxin 3A and 3B in the retina was analyzed by *in situ* hybridization of specific probes derived from the 3' untranslated region of the syntaxin 3A and 3B cDNA (Fig. 4). Sense probes for the same region of mRNA were used as negative controls. The syntaxin 3B antisense probes specifically labeled the outer nuclear layer (ONL), as well as cells in the inner nuclear layer (INL). The ONL contains only cell bodies of the rod and cone photoreceptors confirming that syntaxin 3B is expressed in these ribbon synapse forming cells. The INL contains cell bodies of bipolar cells that form ribbon synapses as well as other cell types such as amacrine cells. Since syntaxin 3B is specifically found in synaptic terminals of bipolar cells it is most likely that the cell bodies labeled in the INL represent bipolar cells.

Some spotty labeling was also seen in the ganglion cell layer. This ganglion cell layer labeling is most likely an artifact, since a similar signal was present in the sense control. No specific signal was detectable using the syntaxin 3A antisense probe, indicating that the expression level of this isoform in the retina is very low, consistent with the results of the RT-PCR analysis. These results indicate that the syntaxin 3 isoform in ribbon synapses of the retina is syntaxin 3B.

Domain structure of Syntaxin 3B

Protein sequences of the mouse syntaxin 3A and syntaxin 3B were aligned with that of syntaxin1A, the isoform found in conventional synapses (Figure 5). Alignment shows that syntaxin 1A, is more homologous to syntaxin 3B (66.6% identity) than it is to the non-neuronal syntaxin 3A (61.2 % identity). Since the two syntaxin 3 isoforms differ only in the second half of the SNARE domain and the transmembrane domain, these two domains were compared. For syntaxin 3B, both of these domains are more similar to syntaxin 1A than to syntaxin 3A. The second half of the SNARE domain of syntaxin 3B is 73.7% identical to the same domain of syntaxin 1A, in comparison to only a 60.5 % identity between the domains of syntaxin 3A and 1A. The highest homology between syntaxin 1A and 3B is in the transmembrane domains (79.2 % identity). In contrast, the transmembrane domain of syntaxin 3A is very different from syntaxin 1A, sharing only 38.5 % identity. Interestingly, two cysteine residues in the transmembrane domain of syntaxin 1A which have been implicated in the interaction between syntaxin 1A and the L-type calcium channel ($Ca_V1.2$) (Arien et al., 2003), are also conserved in syntaxin 3B (C270,C271) but not in syntaxin 3A.

Interaction of syntaxin 3B with other synaptic proteins

The interaction of syntaxin 3B with proteins known to play a role in synaptic vesicle exocytosis was characterized using pulldown experiments with recombinant proteins and mouse retina extract. Recombinant syntaxin 3B was composed of GST fused to the cytoplasmic domain of syntaxin 3B. Since the interaction of syntaxin 1A with many of the proteins involved in exocytosis has been well characterized, GST fused to the cytoplasmic domain of syntaxin 1A was used as a positive control. For a negative control, GST alone was used. The fusion proteins were immobilized on glutathione beads and then incubated with retina extract containing either 150 μM Ca^{2+} or 2 mM EGTA.

NIH-PA Author Manuscript

NIH-PA Author Manuscript

NIH-PA Author Manuscript

Munc-18/n-sec1 is a soluble protein that has been shown to be essential for neurotransmitter release (Verhage et al., 2000). Munc18/n-sec1 has been shown to interact with syntaxin 1A (Hata et al., 1993, Pevsner et al. 1994b).

The pulldown experiment shows that Munc-18/n-sec1 from retina extract interacts with GST-syntaxin 3B (Figure 6). This interaction is independent of the Ca^{2+} concentration. Similar signal intensities on the Western blot indicate that the strength of native Munc-18/n-sec1 interaction with recombinant syntaxin 3B is comparable to the strength of the interaction between native Munc18/n-sec1 and recombinant syntaxin 1A.

One of the three constituents of the synaptic SNARE complex is the presynaptic plasma membrane protein, SNAP-25. *In vitro* binding experiments have shown that SNAP-25 and syntaxin 1A can form a heterodimer (Hayashi et al., 1994; Pevsner et al., 1994a). In agreement with these experiments, SNAP-25 from retina extract can bind GST-syntaxin1A (Fig. 7, lanes 3 and 4) in a Ca2+-independent manner. In contrast to the strong interaction between SNAP-25 and GST-syntaxin 1A, the interaction between GST-syntaxin 3B and SNAP-25 is much weaker (Fig. 7, lanes 1 and 2). This interaction is partially affected by Ca^{2+} concentration with more SNAP-25 bound in elevated Ca2+ concentrations. The results of this experiment suggest that SNAP-25 has a lower affinity for syntaxin 3B than syntaxin 1A.

Next, the interaction between GST-syntaxins and synaptobrevin2/VAMP2 from retina extract was examined. In this experiment we could not detect binding between GST-syntaxin 1A or GST-syntaxin 3B and native synaptobrevin/VAMP2 (data not shown). The results of this experiment are comparable to the finding of Matos and colleagues that binding between synaptobrevin/VAMP2 from brain extract and GST-syntaxin 1A is not detectable (Matos et al., 2003).

Syntaxin 3B can mediate vesicle fusion

To examine if syntaxin 3B can mediate vesicle fusion, a reconstituted liposome fusion assay was utilized (Weber et al., 1998). In this *in vitro* fusion assay, the v-SNARE synaptobrevin/VAMP2 was reconstituted into liposomes containing a mixture of two different fluorescent lipids that contain the fluorophores rhodamine or NBD (7-nitro-2-1,3-benzoxadiazol-4-yl). Under these conditions rhodamine will quench the fluorescence of NBD. The t-SNAREs SNAP-25 and syntaxin 3B (or the positive control syntaxin1A), were reconstituted as a preformed complex into liposomes containing no fluorescent lipids. The reconstituted v-and t-SNARE liposomes were mixed together and incubated overnight at 4° C, allowing the formation of interbilayer complexes without significant fusion (Parlati et al., 1999). The fusion reaction was initiated by raising the temperature to 37 ° C. The dilution of lipids that occurs when a v-SNARE liposome (donor) fuses with a t-SNARE liposome (acceptor) results in dequenching of the fluorophore NBD. This increase in NBD fluorescence (excitation 460 nm, emission 538 nm) is monitored at 2 minute intervals for 120 minutes. Detergent is added in a final step to determine the maximum NBD fluorescence. The kinetic data are normalized as a percent of maximum fluorescence as previously described (Parlati et al., 1999; Scott et al., 2003).

As shown in figure 8A, vesicles reconstituted with SNAP-25 and syntaxin 3B can fuse with vesicles reconstituted with synaptobrevin/VAMP2 (open circles). To ensure that fusion is due to the interaction between synaptobrevin/VAMP2 and the t-SNARE complex, soluble synaptobrevin/ VAMP2 lacking the transmembrane domain was included in the reaction as a negative control. Inclusion of this protein results in inhibition of fusion (Fig. 8A, filled boxes). Comparison of the rate of fusion for syntaxin3B containing t-SNARE vesicles and syntaxin 1A containing t-SNARE vesicles indicates that these reactions proceed at different

NIH-PA Author Manuscript

NIH-PA Author Manuscript

NIH-PA Author Manuscript

rates. Two distinct rates of fusion can be distinguished in this assay: the faster initial fusion rate, thought to represent the fusion of SNARE complexes that have been formed during the overnight incubation (Parlati et al., 1999) and the slower second rate, thought to represent a combination of the rate of SNARE complex formation and the rate of the fusion reaction. The initial fusion rate was determined in the 10 minute time interval between 4 and 14 minutes after raising the temperature to 37°C. Analysis of these data revealed that syntaxin 3B-containing vesicles have an initial fusion rate that is about 2.5 times slower than the initial fusion rate of syntaxin 1A-containing vesicles (Fig. 8B). This slower rate of fusion is not due to fewer SNAP-25/syntaxin 3B complexes, since the amount of SNAP-25/syntaxin 3B reconstituted into vesicles is comparable to the amount of SNAP-25/syntaxin 1A (Fig. 8C). Overall, the results of these *in vitro* fusion assays demonstrate that syntaxin 3 is a functional t-SNARE that can catalyze vesicle fusion together with the neuronal SNAREs SNAP-25 and synaptobrevin2/VAMP2.

DISCUSSION

We show here that syntaxin 3B is the only syntaxin 3 isoform that is expressed in retinal ribbon synapses. Other syntaxin isoforms that get targeted to the plasma membrane (i.e. syntaxins 1, 2 and 4) have been shown to be absent from retinal ribbon synapses (Sherry et al., 2006). Therefore, we conclude that syntaxin 3B most likely mediates synaptic vesicle exocytosis in ribbon synapses in the retina. Previous studies have shown that syntaxin 3 is essential for vesicle transport from the trans-Golgi network to the apical membrane in epithelial cells (Low et al., 1998; Sharma et al., 2006). These experiments used syntaxin 3 antibodies that did not distinguish between the different syntaxin 3 spliceforms as well as recombinant syntaxin 3A. Due to the lack of antibody specificity, it remained unclear which syntaxin 3 isoform is expressed in epithelial cells. We demonstrate here that syntaxin 3A is the only isoform detectable in the kidney; therefore syntaxin 3A is the isoform involved in epithelial cell membrane trafficking.

Besides its presumed role in synaptic vesicle fusion in ribbon synapses, syntaxin 3 has been recently implicated in the trafficking of rhodopsin in rod photoreceptors (Chuang et al., 2007). This study did not distinguish between the different isoforms and used recombinant syntaxin 3A to demonstrate a biochemical interaction between SARA, a rhodopsin interacting protein, and syntaxin 3A. However, we have shown that photoreceptors express syntaxin 3B and not syntaxin 3A. Further binding studies using recombinant syntaxin 3B and SARA will be required to confirm that these two proteins can also interact. In this same study, short hairpin (sh) RNA against syntaxin 3A was used to demonstrate that syntaxin 3 is involved in the trafficking of rhodopsin. The shRNA target sequence was located in the region of the syntaxin3A mRNA transcript which encodes its N-terminal domain. As stated previously, the N-terminal region of syntaxin 3A and 3B is identical. Therefore, it is likely that the shRNA would also affect the syntaxin3B found in the photoreceptors. However the authors of the study only demonstrated the efficiency of the shRNA for syntaxin 3A but not for syntaxin 3B. Further experiments will therefore be required to clarify the role of syntaxin 3B in the trafficking of rhodopsin in rod photoreceptors.

We decided to further investigate the role of syntaxin 3B in synaptic vesicle exocytosis through the characterization of its interaction with native SNARE proteins. In these studies we show that syntaxin3B can bind specifically to Munc18 and SNAP-25 from mouse retina extract. Recombinant syntaxin 3B bound less SNAP-25 than syntaxin 1A, suggesting a difference in binding affinities between the two syntaxin isoforms. To examine the effect of syntaxin 3B on the kinetics of membrane fusion, *in vitro* liposome fusion assays were performed. These assays indicate that vesicles containing syntaxin 3B and SNAP-25 can efficiently fuse with vesicles containing synaptobrevin2/VAMP2. However, the initial rate

NIH-PA Author Manuscript

NIH-PA Author Manuscript

NIH-PA Author Manuscript

of fusion catalyzed by the syntaxin3B containing t-SNARE vesicles is approximately half the rate of fusion for syntaxin 1A containing t-SNARE vesicles. It should be pointed out that the fusion rates observed in the liposome fusion assay are much slower than the rates observed for synaptic vesicle exocytosis. This is probably due to the fact that the fusion of synaptic vesicles is modulated by a variety of other proteins, such as synaptotagmin, complexins and Munc18/n-sec1. Therefore, it is difficult to compare the fusion rates observed in our experiments to the rates of synaptic vesicle exocytosis *in vivo*. Nevertheless, it is interesting to note that the fusion rate measured in ribbon synapses differs from the fusion rate measured in non ribbon-type synapses. The rate constant of synaptic vesicle fusion in ribbon synapses of goldfish rod bipolar cells (Heidelberger et al., 1994) has been determined to be approximately half of the rate constant of synaptic vesicle fusion in the rat calyx of Held (a non ribbon synapse) (Schneggenburger and Neher, 2000). Direct comparison of these two fusion rates is problematic because these experiments were performed using two different species. However, the different biochemical properties of the syntaxins found in these two synapse types might contribute to the differences in vesicle fusion rate.

What could be the molecular basis for the difference in SNAP-25 binding and fusion rates between syntaxin 1A and syntaxin 3B? It is known that syntaxin 1A can exist in an open or closed conformation (Dulubova et al., 1999). Only the open conformation can interact with SNAP-25. In the closed conformation the N-terminus interacts with the SNARE domain and prevents interaction with other SNARE proteins. A likely explanation for the decreased SNAP-25 binding and reduced fusion rate of syntaxin3B is that more syntaxin 3B in the closed conformation than syntaxin 1A. This idea is consistent with the fact that the N-terminal domain of syntaxin 3B is the part of the protein that is most divergent from the corresponding region of syntaxin 1A. In addition to conformational differences between syntaxin 1A and 3B, other proteins specific to the synapse type could affect rate of fusion *in vivo*. Syntaxin 3B may require another co-factor to bind SNAP-25 efficiently and catalyze fusion. Potential candidates for such a factor would be the complexins, a group of four related proteins (complexins I, II, III and IV) that bind the SNARE complex. The complexins are essential for Ca2+ regulated synaptic vesicle exocytosis (McMahon et al., 1995; Reim et al., 2001; Chen et al., 2002). Interestingly, ribbon synapses in the retina contain a set of complexin isoforms distinct from conventional synapses. Ribbon synapses of the retina contain complexins III and IV, while complexins I and II are found in conventional synapses (Reim et al., 2005). Since the three dimensional structure of the synaptic SNARE/complexin I complex is known we compared the part of syntaxin 1 that interacts with complexin 1 (residues 214-232) to the corresponding region in syntaxin 3B. All the residues of syntaxin 1 that interact directly with complexin 1 (M215, D218, L222 and M229) are conserved in syntaxin 3B (Chen et al., 2002), indicating that syntaxin 3B may also interact with complexin 1. Furthermore pulldown experiments using immobilized GST-complexins and retina extract have demonstrated that complexins I, III and IV can bind syntaxin 3 from retina (i.e. syntaxin3B) (Reim et al., 2005). Therefore, it is likely that complexins 3 and 4 interact with syntaxin 3B to catalyze efficient vesicle fusion.

Acknowledgments

We thank Dr. Ruth Heidelberger and Diana Lazzell for helpful discussions. We thank Nataliia Bogdanova for excellent technical assistance. We thank Dr. Hui-Chen Lu for the use of her microscope.

This work was supported by NIH EY016452 (R.J.), NIH GM071832 (J.A.M.) and the Mental Retardation and Developmental Disabilities Research Center, *in situ* hybridization core lab at Baylor College of Medicine (HD024064 C3). Leigh Curtis was supported by training grant NIH T32 NS007467. The content is solely the responsibility of the authors and does not necessarily represent the official views of the National Institutes of Health.

NIH-PA Author Manuscript

NIH-PA Author Manuscript

NIH-PA Author Manuscript

Literature Cited

Arien H, Wiser O, Arkin IT, Leonov H, Atlas D. Syntaxin 1A modulates the voltage-gated L-type calcium channel (Ca(v)1.2) in a cooperative manner. J Biol Chem. 2003; 278:29231–29239. [PubMed: 12721298]

Belizaire R, Komanduri C, Wooten K, Chen M, Thaller C, Janz R. Characterization of synaptogyrin 3 as a new synaptic vesicle protein. J Comp Neurol. 2004; 470:266–281. [PubMed: 14755516]

Bennett MK, Garcia-Arraras JE, Elferink LA, Peterson K, Fleming AM, Hazuka CD, Scheller RH. The syntaxin family of vesicular transport receptors. Cell. 1993; 74:863–873. [PubMed: 7690687]

Brandstätter JH, Wässle H, Betz H, Morgans CW. The plasma membrane protein SNAP-25, but not syntaxin, is present at photoreceptor and bipolar cell synapses in the rat retina. Eur J Neurosci. 1996; 8:823–828. [PubMed: 9081634]

Bruns D, Engers S, Yang C, Ossig R, Jeromin A, Jahn R. Inhibition of transmitter release correlates with the proteolytic activity of tetanus toxin and botulinus toxin a in individual cultured synapses of hirudo medicinalis. J of Neurosci. 1997; 17:1898–1910. [PubMed: 9045719]

Catterall WA. Interactions of presynaptic Ca2+ channels and snare proteins in neurotransmitter release. Ann N Y Acad Sci. 1999; 868:144–159. [PubMed: 10414292]

Chen X, Tomchick DR, Kovrigin E, Arac D, Machius M, Südhof TC, Rizo J. Three-dimensional structure of the complexin/SNARE complex. Neuron. 2002; 33:397–409. [PubMed: 11832227]

Chuang JZ, Zhao Y, Sung CH. SARA-regulated vesicular targeting underlies formation of the light-sensing organelle in mammalian rods. Cell. 2007; 130:535–547. [PubMed: 17693260]

Dulubova I, Sugita S, Hill S, Hosaka M, Fernandez I, Südhof TC, Rizo J. A conformational switch in syntaxin during exocytosis: role of munc18. EMBO J. 1999; 18:4372–4382. [PubMed: 10449403]

Fili O, Michaelevski I, Bledi Y, Chikvashvili D, Singer-Lahat D, Boshwitz H, Linial M, Lotan I. Direct interaction of a brain voltage-gated K+ channel with syntaxin 1A: functional impact on channel gating. J Neurosci. 2001; 21:1964–1974. [PubMed: 11245681]

Hata Y, Slaughter CA, Südhof TC. Synaptic vesicle fusion complex contains unc-18 homologue bound to syntaxin. Nature. 1993; 366:347–351. [PubMed: 8247129]

Hayashi T, McMahon H, Yamasaki S, Binz T, Hata Y, Südhof TC, Niemann H. Synaptic vesicle membrane fusion complex: action of clostridial neurotoxins on assembly. EMBO J. 1994; 13:5051–5061. [PubMed: 7957071]

Heidelberger R, Heinemann C, Neher E, Matthews G. Calcium dependence of the rate of exocytosis in a synaptic terminal. Nature. 1994; 371:513–515. [PubMed: 7935764]

Heidelberger R, Thoreson WB, Witkovsky P. Synaptic transmission at retinal ribbon synapses. Prog Retin Eye Res. 2005; 24:682–720. [PubMed: 16027025]

Ibaraki K, Horikawa HP, Morita T, Mori H, Sakimura K, Mishina M, Saisu H, Abe T. Identification of four different forms of syntaxin 3. Biochem Biophys Res Commun. 1995; 211:997–1005. [PubMed: 7598732]

Jahn R, Scheller RH. SNAREs--engines for membrane fusion. Nat Rev Mol Cell Biol. 2006; 7:631–643. [PubMed: 16912714]

Low SH, Chapin SJ, Wimmer C, Whiteheart SW, Komuves LG, Mostov KE, Weimbs T. The SNARE machinery is involved in apical plasma membrane trafficking in MDCK cells. J Cell Biol. 1998; 141:1503–1513. [PubMed: 9647644]

Matos MF, Mukherjee K, Chen X, Rizo J, Südhof TC. Evidence for SNARE zippering during Ca2+-triggered exocytosis in PC12 cells. Neuropharmacology. 2003; 45:777–786. [PubMed: 14529716]

McMahon HT, Missler M, Li C, Südhof TC. Complexins: cytosolic proteins that regulate SNAP receptor function. Cell. 1995; 83:111–109. [PubMed: 7553862]

Morgans CW, Brandstätter JH, Kellerman J, Betz H, Wässle H. A SNARE complex containing syntaxin 3 is present in ribbon synapses of the retina. J Neurosci. 1996; 16:6713–6721. [PubMed: 8824312]

Parlati F, Weber T, McNew JA, Westermann B, Sollner TH, Rothman JE. Rapid and efficient fusion of phospholipid vesicles by the alpha-helical core of a SNARE complex in the absence of an N-terminal regulatory domain. Proc Natl Acad Sci U S A. 1999; 96:12565–12570. [PubMed: 10535962]

NIH-PA Author Manuscript

NIH-PA Author Manuscript

NIH-PA Author Manuscript

Pevsner J, Hsu SC, Braun JE, Calakos N, Ting AE, Bennett MK, Scheller RH. Specificity and regulation of a synaptic vesicle docking complex. Neuron. 1994a; 13:353–361. [PubMed: 8060616]

Pevsner J, Hsu SC, Scheller RH. n-Sec1: a neural-specific syntaxin-binding protein. Proc Natl Acad Sci U S A. 1994b; 91:1445–1449. [PubMed: 8108429]

Reim K, Mansour M, Varoqueaux F, McMahon HT, Südhof TC, Brose N, Rosenmund C. Complexins regulate a late step in Ca2+-dependent neurotransmitter release. Cell. 2001; 104:71–81. [PubMed: 11163241]

Reim K, Wegmeyer H, Brandstätter JH, Xue M, Rosenmund C, Dresbach T, Hofmann K, Brose N. Structurally and functionally unique complexins at retinal ribbon synapses. J Cell Biol. 2005; 169:669–680. [PubMed: 15911881]

Schneggenburger R, Neher E. Intracellular calcium dependence of transmitter release rates at a fast central synapse. Nature. 2000; 406:889–893. [PubMed: 10972290]

Scott BL, Van Komen JS, Liu S, Weber T, Melia TJ, McNew JA. Liposome fusion assay to monitor intracellular membrane fusion machines. Methods Enzymol. 2003; 372:274–300. [PubMed: 14610819]

Sharma N, Low SH, Misra S, Pallavi B, Weimbs T. Apical targeting of syntaxin 3 is essential for epithelial cell polarity. J Cell Biol. 2006; 173:937–948. [PubMed: 16785322]

Sheng ZH, Rettig J, Takahashi M, Catterall WA. Identification of a syntaxin-binding site on N-type calcium channels. Neuron. 1994; 13:1303–1313. [PubMed: 7993624]

Sherry DM, Mitchell R, Standifer KM, du PB. Distribution of plasma membrane-associated syntaxins 1 through 4 indicates distinct trafficking functions in the synaptic layers of the mouse retina. BMC Neurosci. 2006; 7:54. [PubMed: 16839421]

Singer-Lahat D, Sheinin A, Chikvashvili D, Tsuk S, Greitzer D, Friedrich R, Feinshreiber L, Ashery U, Benveniste M, Levitan ES, Lotan I. K+ channel facilitation of exocytosis by dynamic interaction with syntaxin. J Neurosci. 2007; 27:1651–8. [PubMed: 17301173]

Sterling P, Matthews G. Structure and function of ribbon synapses. Trends Neurosci. 2005; 28:20–29. [PubMed: 15626493]

Verhage M, Maia AS, Plomp JJ, Brussaard A, Heeroma JH, Vermeer H, Toonen RF, Hammer RE, van der Berg TK, Missler M, Geuze HJ, Südhof TC. Synaptic Assembly of the Brain in the Absence of Neurotransmitter Secretion. Science. 2000; 287:864–869. [PubMed: 10657302]

Von Kriegstein K, Schmitz F, Link E, Südhof TC. Distribution of synaptic vesicle proteins in the mammalian retina identifies obligatory and facultative components of ribbon synapses. Eur J Neurosci. 1999; 11:1335–1348. [PubMed: 10103129]

Yaylaoglu MB, Titmus A, Visel A, Alvarez-Bolado G, Thaller C, Eichele G. Comprehensive expression atlas for fibroblast growth factors and their receptors generated by a novel in situ hybridization platform. Dev Dyn. 2005; 234:371–386. [PubMed: 16123981]

Weber T, Zemelman BV, McNew JA, Westermann B, Gmachl M, Parlati F, Sollner TH, Rothman JE. SNAREpins: minimal machinery for membrane fusion. Cell. 1998; 92:759–772. [PubMed: 9529252]

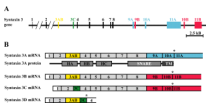

Fig. 1. Different syntaxin 3 isoforms are generated by differential splicing of the syntaxin3 gene

A. The exon/intron structure of the gene is depicted with exons labeled by numbers. Differentially spliced exons are depicted in different colors that correspond to the differential spliced mRNAs depicted below: exon 3AB, yellow; exon 3C, green, exon 9A, 10A, 11A, blue; exon 9B, 10B, 11B, red. B. Structure of the mRNAs of the different isoforms of syntaxin 3. The position of the different exons in the mRNA is depicted. The same colors as in A. are used to label the different exons. The position of the stop codons at the end of the translated regions are marked by an asterisk. The domain structure of the syntaxin3A protein is shown underneath the corresponding mRNA. The different domains are of the protein are marked: HA, HB and HC domains (HA, HB, HC), SNARE domain (SNARE), transmembrane domain (TM).

NIH-PA Author Manuscript NIH-PA Author Manuscript NIH-PA Author Manuscript

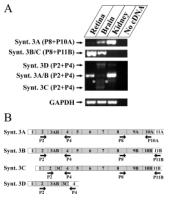

Fig. 2. Syntaxin 3B is the syntaxin 3 isoform expressed in the retina

A. RT-PCR analysis of the expression of different syntaxin isoforms in different tissues. Arrows mark the position of the specific bands generated by the indicated primers (P2, P4, P8, P10A). Asterisks mark nonspecific PCR products. B. The location of the PCR primers in relation to the mRNAs of the different syntaxin 3 isoforms is indicated. The different exons are marked and the predicted coding region is shaded.

NIH-PA Author Manuscript
NIH-PA Author Manuscript
NIH-PA Author Manuscript

NIH-PA Author Manuscript

NIH-PA Author Manuscript

NIH-PA Author Manuscript

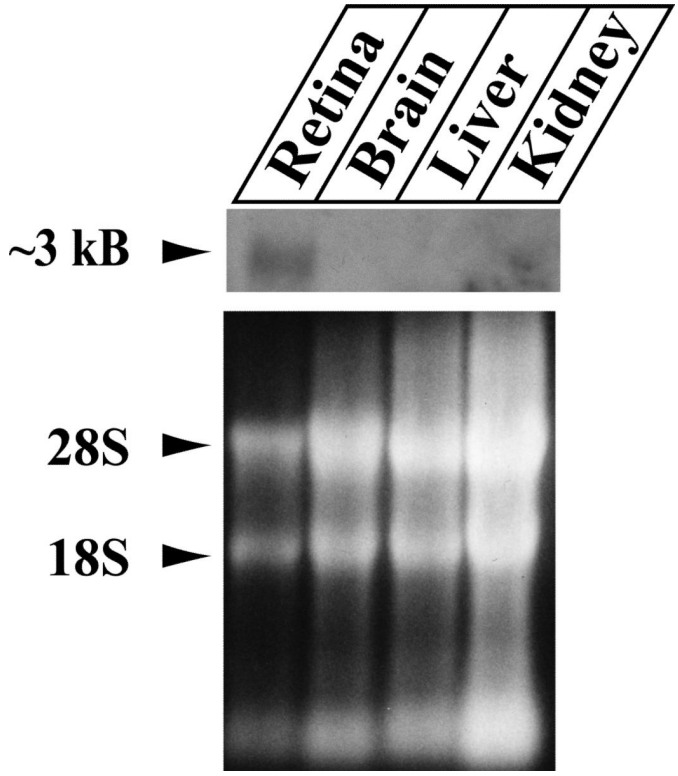

Fig. 3. Analysis of the tissue distribution of syntaxin3B mRNA

Top panel: Expression of syntaxin 3B mRNA in different tissues was analyzed by Northern blot using a probe specific for syntaxin 3B. Bottom panel: Total RNA separated on denaturing/formaldehyde gel and stained with ethidium bromide. The presence of distinct ribosomal 28S and 18S bands demonstrates that the RNA is not degraded.

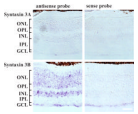

Fig. 4. Syntaxin 3B is expressed in ribbon synapse- forming neurons in the retina

Antisense riboprobes (left panel) specific for the syntaxin 3A (top panel) and syntaxin 3B (bottom panel) were used to analyze the mRNA distribution in the mouse retina by in situ hybridization. The different layers of the retina are labeled on the left [outer nuclear layer (ONL), outer plexiform layer (OPL), Inner nuclear layer (INL), inner plexiform layer (IPL) and ganglion cell layer (GCL)]. Sense probes were used as negative controls (right panel). Antisense probes for syntaxin 3B label the cell bodies of neurons in the ONL and the INL. Scale bar = 100 μm

NIH-PA Author Manuscript NIH-PA Author Manuscript NIH-PA Author Manuscript

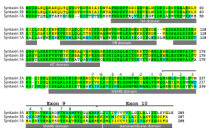

Fig. 5. Sequence alignement of the different syntaxin isoforms

The protein sequences of mouse syntaxin 3A, syntaxin 3B and syntaxin 1A have been aligned for maximal homology. Sequences are identified on the left and residues numbered on the right. Residues that are conserved in all three isoforms are labeled with green background. Residues conserved between two of the syntaxin isoforms are labeled with yellow background. Conservative exchanged residues are labeled with blue background. The position of the differential spliced exons is marked above the sequence. The positions of the hydrophobic interacting layers are numbered in relation to the glutamine (Q) of the central 0 layer.

NIH-PA Author Manuscript NIH-PA Author Manuscript NIH-PA Author Manuscript

NIH-PA Author Manuscript

NIH-PA Author Manuscript

NIH-PA Author Manuscript

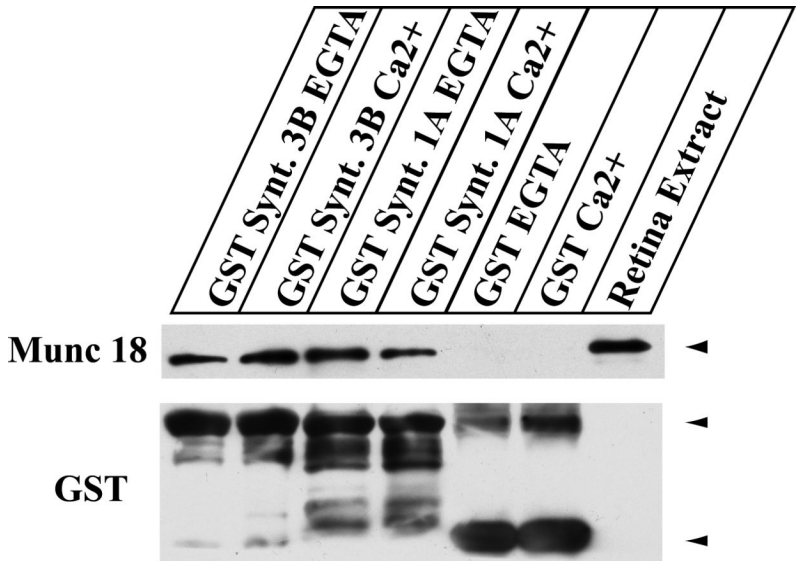

Fig. 6. Munc-18/n-sec1 binds to both syntaxin 1A and syntaxin 3B

Lane 1: Retina extract alone. Lanes 2-3: For a negative control, GST bound to glutathione-sepharose beads was incubated with extract that had either 150 μM calcium or 2 mM EGTA added to it. Lanes 4-7: Retina extract with either 150 μM calcium or 2 mM EGTA was incubated with the indicated GST-fusion proteins (GST-syntaxin 1A and GST-syntaxin 3B). Membrane was probed with an antibody to GST to ensure that the amount of fusion protein in each pulldown was comparable (results below Munc-18/n-sec1 blot).

NIH-PA Author Manuscript

NIH-PA Author Manuscript

NIH-PA Author Manuscript

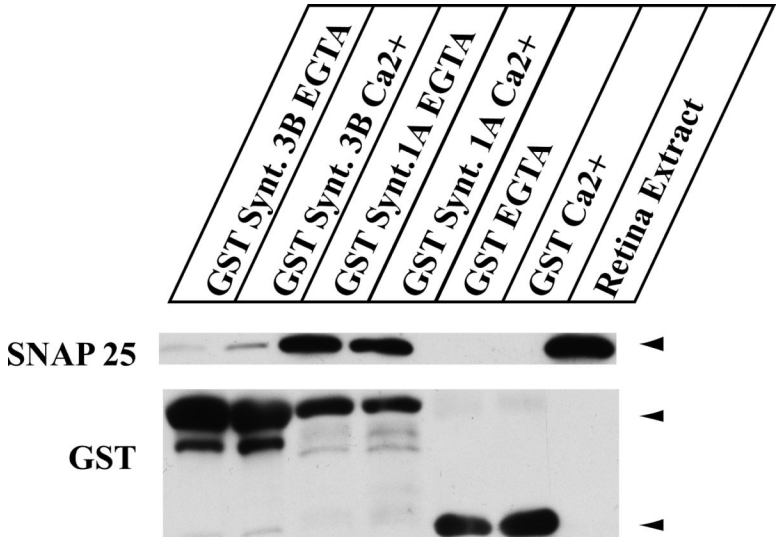

Fig. 7. SNAP-25 binds weakly to syntaxin 3B

Lane 1: Retina extract alone. Lanes 2-3: For a negative control, GST bound to glutathione sepharose beads was incubated with extract that had either 150 μM calcium or 2 mM EGTA added to it. Lanes 4-7: Retina extract with either 150 μM calcium or 2 mM EGTA was incubated with the indicated GST-fusion proteins (GST-syntaxin 1A and GST-syntaxin 3B). Membrane was probed with antibody to GST to ensure that the amount of fusion protein in each pulldown was comparable (results below SNAP-25 blot).

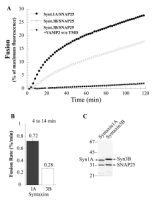

Fig. 8. Syntaxin 3B/SNAP-25 forms a functional SNARE complex

A. Liposomes containing either syntaxin 1A/SNAP-25 (filled circles) or syntaxin 3B/SNAP-25 (open circles) t-SNARE complexes were mixed with v-SNARE liposomes containing synaptobrevin/VAMP2. Background levels of fusion were determined by including soluble synaptobrevin/VAMP2 (VAMP2 w/o TMD, filled box) to reactions containing syntaxin 3B/SNAP-25. Lipid mixing was monitored as an increase in NBD fluorescence for 120 minutes. Fusion is represented as percent maximum fluorescence obtained following detergent solubilization of the liposomes. B. Histogram showing initial fusion rate from 4 to 14 minutes of the t-SNARE liposomes containing either syntaxin1A/SNAP-25 or syntaxin 3B/SNAP-25. C. Five microliters of liposomes containing each complex were run on a 12% SDS-PAGE gel and stained with Coomassie blue.

NIH-PA Author Manuscript NIH-PA Author Manuscript NIH-PA Author Manuscript